THE JOURNAL OF BIOLOGICAL CHEMISTRY VOL. 289, NO. 1, pp. 510–519, January 3, 2014

Angiopoietin-2 Secretion by Endothelial Cell Exosomes

*REGULATION BY THE PHOSPHATIDYLINOSITOL 3-KINASE (PI3K)/Akt/ENDOTHELIAL NITRIC OXIDE SYNTHASE (eNOS) AND SYNDECAN-4/SYNTENIN PATHWAYS**

Received for publication, August 1, 2013, and in revised form, November 12, 2013 Published, JBC Papers in Press, November 14, 2013, DOI 10.1074/jbc.M113.506899

Rong Ju[‡1], Zhen W. Zhuang[‡], Jiasheng Zhang[‡], Anthony A. Lanahan[‡], Themis Kyriakides[§], William C. Sessa[¶], and Michael Simons[‡‖2]

From the [‡]Yale Cardiovascular Research Center, Section of Cardiovascular Medicine, Department of Internal Medicine, [§]Department of Pathology, [¶]Department of Pharmacology, and [‖]Department of Cell Biology, Yale University School of Medicine, New Haven, Connecticut 06520

Background: Angiopoietin-2 (Ang2) is a secreted Tie2 ligand involved in regulation of vascular homeostasis.
Results: Ang2 is secreted in exosomes. This process is negatively controlled by PI3K/Akt/eNOS and positively by the syndecan-4/syntenin pathway. Syndecan-4 knock-out partially rescues vascular defects in Akt1$^{-/-}$ mice.
Conclusion: Exosomal Ang2 secretion is regulated by the PI3K/Akt/eNOS and syndecan-4/syntenin pathways.
Significance: This study describes a novel mechanism of endothelial Ang2 secretion.

Angiopoietin-2 (Ang2) is an extracellular protein and one of the principal ligands of Tie2 receptor that is involved in the regulation of vascular integrity, quiescence, and inflammation. The mode of secretion of Ang2 has never been established, however. Here, we provide evidence that Ang2 is secreted from endothelial cells via exosomes and that this process is inhibited by the PI3K/Akt/endothelial nitric oxide synthase (eNOS) signaling pathway, whereas it is positively regulated by the syndecan-4/syntenin pathway. Vascular defects in Akt1 null mice arise, in part, because of excessive Ang2 secretion and can be rescued by the syndecan-4 knock-out that reduces extracellular Ang2 levels. This novel mechanism connects three critical signaling pathways: angiopoietin/Tie2, PI3K/Akt/eNOS, and syndecan/syntenin, which play important roles in vascular growth and stabilization.

Vascular morphogenesis and homeostasis are complex biological processes tightly controlled by multiple signaling pathways. Among these, the angiopoietin/Tie2 signaling pathway has gained increasing attention in the past decade (1). Angiopoietin-1 (Ang1)[3] is secreted primarily from perivascular cells and activates Tie2 and its downstream targets leading to stabilization and maturation of blood vessel. Angpoietin-2 (Ang2) is produced primarily by endothelial cells and functions largely as a Tie2 antagonist, destabilizing established vasculature by interfering with Ang1 function (2, 3). However, under certain circumstances, Ang2 can also serve as an agonist and activate Tie2 (4, 5). Despite numerous studies dealing with Ang2 function and transcriptional regulation, little is known about regulation of its secretion (6, 7).

Recently, certain growth factors such as Wnt (8) have been reported to be secreted via exosomes. Exosomes are small membrane vesicles containing proteins, mRNAs, and microRNAs that are believed to function in mediating intercellular communications (reviewed in (9)). Exosomes originate from intraluminal vesicles that are generated by inward budding of endosomes to form multivesicular bodies, a process regulated by the ESCRT (endosomal-sorting complex required for transport) machinery (reviewed in Ref. 10). Recently, Baietti *et al.* (11) reported that the syndecan-1,-4·syntenin complex is essential for exosome biosynthesis. This occurs due to interaction of the syndecan·syntenin complex with Alix, an ESCRT III-binding protein. Knockdown of syndecan-1, syndecan-4, or syntenin results in decreased exosome production (11).

Syndecans belong to a four-member family of transmembrane proteoglycans (12). All syndecans possess a highly homologous intracellular domain with a PDZ motif at their C-terminal ends, which binds PDZ domain-containing proteins that include synectin (13) and syntenin (14). Interactions of syndecan-4 and its cytoplasmic partners synectin and syntenin have been shown to be essential for the activation Rac1 and RhoG, thereby regulating cell migration (15, 16), integrin recycling (17, 18), as well as exosome biosynthesis (11).

We have previously demonstrated that syndecan-4 regulates the PI3K/Akt signaling pathway (19, 20) that in turn regulates both pathological and physiological angiogenesis at multiple levels (reviewed in Ref. 21). However, the precise mechanisms underlying the PI3K/Akt regulation of angiogenesis remain unclear. One possibility is that this involves regulation of Ang2 release. This is suggested by the observations that Akt1 null mice have profound angiogenesis defects in both physiological and pathological settings (22, 23) that can be rescued by expression of constitutively activated eNOS (24), one of the major downstream targets of Akt1. NO, the product of eNOS activa-

* This work was supported in part by National Institutes of Health Grants R01 HL062289 (to M. S.) and PO1 HL107205 (to M. S., T. K., and W. C. S.)
[1] Present address: State Key Laboratory of Ophthalmology, Zhongshan Ophthalmic Center, Sun Yat-Sen University, Guangzhou 510060, China.
[2] To whom correspondence should be addressed: Yale Cardiovascular Research Center, Sect. of Cardiovascular Medicine, Dept. of Internal Medicine, Yale University School of Medicine, 300 Cedar St., New Haven, CT 06520. Tel.: 203-785-7000; Fax: 203-785-5144; E-mail: michael.simons@yale.edu.
[3] The abbreviations used are: Ang1, angiopoietin-1; S4, syndecan-4; HUVEC, human umbilical vein endothelial cells; eNOS, endothelial nitric oxide synthase; DKO, double knockout.

tion, was shown to control secretion of von Willebrand factor from Weibel-Palade bodies (25), which also contain Ang2 (6). In addition, Tsigkos *et al.* (7) reported that the phosphatase and tensin homolog (PTEN)/PI3K/Akt pathway regulates Ang2 release. These observations led us to hypothesize that the PI3K/Akt1-dependent stimulation of NO production via eNOS suppresses secretion of Ang2, thus accounting for eNOS-mediated rescue of angiogenic defects seen in $Akt1^{-/-}$ mice.

To test this hypothesis and to understand the role of syndecans in Ang2 action, we investigated the mechanisms regulating Ang2 secretion and the corresponding *in vivo* vascular phenotypes. We find that Ang2 is secreted from endothelial cells via exosomes. The release of exosomal Ang2 is increased by either the knock-out or knockdown of Akt1 or the inhibition of either PI3 kinase or eNOS. Conversely, knock-out or knockdown of syndecan-4 or syntenin decreases secretion of exosomal Ang2. In agreement with the opposing roles of these two pathways, we observed that vascular defects found in $Akt1^{-/-}$ mice, which include reduced coronary arterioles, reduced blood flow recovery following hind limb ischemia, and impaired retinal vasculature development, were all rescued in Akt1/syndecan-4 double knock-out mice, suggesting a genetic interaction among the PI3K, syndecan-4/syntenin, and Ang2 pathways.

MATERIALS AND METHODS

Reagents and Antibodies—Goat antibody against angiopoietin-2 (F-18) and mouse antibody against p-Tyr (PY99) were purchased from Santa Cruz Biotechnology. Rabbit anti-human von Willebrand factor antibody was from DAKO. Rabbit antibodies against CD63 and Calnexin were purchased from Epitomics. Anti-syntenin and anti-syndecan-4 were from Abcam. Antibodies against Tie2, Akt, and Akt-Ser-473 were from Cell Signaling Technology. Anti-Tie2 antibody and angiopoietin-1 and -2 were purchased from R&D Systems. Anti-α-tubulin and anti-β-actin antibodies were purchased from Sigma. Isolectin B4 and secondary antibodies were purchased from Molecular Probes (Invitrogen). HUVEC cells were purchased from the tissue core laboratory at Yale University. Medium 199, DMEM, and Lipofectamine RNAiMAX as well as Lipofectamine 2000 were from Invitrogen. siRNAs against human Ang2, S2, S4, Akt1, syntenin were obtained from OriGene. LY294002 and L-NAME were purchased from Sigma. Endothelial cell growth supplement was purchased from Biomedical Technologies.

Cell Culture and siRNA Transfection—Mouse primary endothelial cells were isolated from lung as described previously (19) and maintained in DMEM supplemented with 20% FBS, nonessential amino acid, sodium pyruvate, penicillin, streptomycin at standard concentrations. HUVEC cells were cultured in medium 199 with 20% FBS and endothelial cell growth supplement. Both types of cells were cultured at 37 °C in 5% CO_2.

siRNAs were transfected into endothelial cells, either mouse lung endothelial cells or HUVEC, with Lipofectamine RNAiMAX (Invitrogen) according to the manufacturer's protocols. The transfected cells were cultured for 48 to 72 h before they were used for the experiments.

Exosome Isolation, Fractionation, and Characterization—Endothelial cells were cultured and reached to confluency. Then the completed medium was replaced with DMEM containing 0.5% exosome-depleted FBS unless described otherwise. The conditioned media were collected 12–24 h later. Exosomes were isolated from the media according to the standard protocol with minor modification (26). In brief, exosomes were isolated by four sequential centrifugations: 10 min at 300 × *g*; 10 min at 2000 × *g*; 30 min at 10,000 × *g*, and 90 min at 100,000 × *g*. The exosome pellets were suspended in PBS, pelleted by 100,000 × *g* for 70 min. The final pellets were resuspended either in PBS or 1× SDS gel loading buffer (Boston Bioproducts). Corresponding cells were washed with PBS and lysed in PIPES or radioimmune precipitation assay buffer (Boston Bioproducts) supplemented with protease inhibitor mixture (Roche Applied Science) and phosphatase inhibitor mixture (Roche Applied Science). The protein concentration was determined by BCA Protein assay kit (Thermo Scientific), and the corresponding exosome preparations were adjusted accordingly.

Exosome fractionation was performed as described with modifications (11). Briefly, a 5–40% OptiPrep (Axis-Shield POC) gradient was made according to the manufacturer's instructions. Exosomes (100,000 × *g* pellet) were suspended in 2 ml of 60% OptiPrep, loaded into the bottom of gradient and centrifuged for 16 h at 140,000 × *g*. Fractions were collected at 1 ml per fraction from top to bottom. To concentrate the fractions, each fraction was diluted with PBS by three times, centrifuged at 100,000 for 70 min, and suspended in 1× SDS loading buffer.

Proteinase K Protection Assay—The 100,000 × *g* exosome pellet was resuspended in 10 mM Tris-HCl, pH 7.4, and then 60-μl aliquots were either left untreated or treated with 100 ng of proteinase K (Roche Applied Science) in the presence or absence of 0.5% Triton X-100 for 1 h at 37 °C. The reaction was terminated with phenylmethylsulfonyl fluoride (5 mM final concentration) and Complete protease inhibitor (Roche Applied Science). SDS loading buffer was added, and the samples were heated at 100 °C and analyzed by SDS-PAGE and Western blotting.

Cell Lysis and Western Blot—Cells were lysed in PIPES lysis buffer (25 mM PIPES, pH 7.0, 150 mM NaCl, 5 mM EDTA, and 1% Nonidet P-40) or radioimmune precipitation assay buffer (50 mM Tris-HCl, 150 mM NaCl, 1% Nonidet P-40, 0.5% sodium deoxycholate, and 0.1% SDS together with protease inhibitor mixture (Roche Applied Science) and phosphatase inhibitor mixture (Roche Applied Science). The protein concentration was determined by BCA protein assay kit (Thermo Scientific). The cell lysates were suspended in the reducing SDS sample buffer (Boston BioProducts) and subjected to SDS-PAGE (4–15% Criterion TGX Precast Gel, Bio-Rad Laboratories). The proteins were transferred to PVDF membrane, blocked with 5% milk, and blotted with primary and HRP-conjugated secondary antibodies. The Western signals were visualized with G:BOX (Syngene).

Mice—Syndecan-4-deficient mice (27) and Akt1-deficient mice (28) were crossed to generate Akt1/S4 double KO mice. Both of these strains were C57/Bl6 background.

Immunohistochemistry of Whole-mount Retinas—P5 pups were killed, and the eyes were removed and prefixed in 4% para-

formaldehyde for 20 min at room temperature. The retinas were dissected out and blocked overnight at 4 °C in blocking buffer (0.1 M Tris-HCl, 150 mM NaCl, 1% blocking reagent (PerkinElmer Life Science), and 0.5% Triton X-100). After washing with Pblec (1 mM $MgCl_2$, 1 mM $CaCl_2$, 0.1 mM $MnCl_2$, and 1% Triton X-100 in PBS), the retinas were incubated with isolectin B4 in Pblec overnight followed by incubation with the corresponding secondary antibody for 2 h at room temperature. Then, the retinas were mounted in fluorescent mounting medium (DAKO, Carpinteria, CA). Images were acquired with a PerkinElmer UltraVIEW VoX spinning disc confocal microscope.

Hind Limb Surgery and Laser Doppler Imaging—Hind limb ischemia surgical models were provided by the Microsurgery Core at the Yale Cardiovascular Research Center. Briefly, mice were anesthetized by intraperitoneal injection of ketamine/xylazine (100 mg/10 kg) solution. The femoral artery was ligated at two positions spaced 5-mm apart, with one just below the inguinal ligament and the second distal to superficial epigastric artery. All of the branches between the two ligatures were ligated, and the femoral artery segment was excised. Tissue perfusion was assessed pre- and post-artery ligation, additionally on postoperative days 3, 7, 14, 21, and 28. Flow images of the foot were acquired using a Moor Laser Doppler Imager (Moor Instruments, Ltd.) at 37 ± 0.5 °C under ketamine/xylazine (100 mg/10 kg) anesthesia. The data were analyzed with Moor Laser Doppler Imager image processing software (version 5.3) and reported as the ratio of flow in the left/right hind limb.

Micro-CT Angiography—4–5 pups of each genotype at neonatal day 7 were used. Postnatal day 7 pups were individually heparinized (APP Pharmaceuticals, NDC 63323-540-31) by intraperitoneal injection (50 μl/mouse, 1000 units/ml) and anesthetized by 3–5% isoflurane inhalation according to approved institutional protocols. Surgical procedures were conducted to prepare the mice for a postmortem intracoronary perfusion and contrast agent injection. Briefly, the heart was immediately isolated and connected to a simplified Langendorff perfusion system. A polyethylene tube (PE10, Becton Dickson, catalog no. 427401) was inserted into the left ventricle via the aortic valve to remove the left ventricle load and withdraw back to the ascending aorta. The heart was arrested at the end of diastole through brief perfusion of KCl (100 mM) (29) and was immediately flushed by switching the perfusion solution to 1 ml of warm saline (37 °C), followed by 100 μl of adenosine (3 mg/ml) and 1 ml of 4% neutral paraformaldehyde. Then, the perfusion was changed to 30–50 μl of 20% bismuth (37 °C in 5% gelatin) (30) from the nearest port of the circuit. The perfusion pressure was set at 90–110 mm Hg for 3 s. The whole heart was quickly immersed in a cold saline-circulation bath (0 °C) for 3 min, so that the contrast medium solidified under the perfusion pressure. Finally, the heart was removed and immersed in 2% paraformaldehyde (4 °C) overnight. The achievement of complete filling of the microvasculature by the contrast medium and the microperfusion pattern were examined using a stereoscopic microscope.

A high-resolution, volumetric micro-CT scanner (GE eXplore Locus SP, GE Healthcare) was used to scan the heart with an 8-μm isometric voxel resolution. Micro-CT was operated with 60 kVp x-ray tube voltage, a 100-μA tube current, 2960-ms exposure time per view, 1 × 1 detector binning model, 360° angle, and 0.5° increments per view. Scan time ranged from 2.5 h.

Microview software (GE Healthcare) was used to reconstruct raw data with 8 × 8 × 8 μm^3 voxels, and images were calibrated by the standard radio-attenuation values (air, water, and bone). The initial reconstructed micro-CT data were saved as free view point video format and then transferred to the Advanced Work station (AW4.4, GE Healthcare) for segmentation. Detailed morphometric data on the diameters, area, number of vessels, and distributions of different sized vessels were extracted using modified software (ImageJ; Bethesda, MD). The distribution of the relative arterial vessel number was semi-automatically calculated with a built-in algorithm. Data are expressed as a vascular segmental number, representing the total number of vessels, of a specified diameter, counted in the whole heart.

Electronic Microscope Analysis of Exosomes—Preparation and imagining of exosomes were performed according to the standard protocol (26) with modifications. Then, the 100,000 × *g* pellets containing exosomes from the mouse lung primary endothelial cells were fixed with 2% paraformaldehyde and deposited on Formvar carbon-coated EM grids. The grids were washed with PBS and were further fixed with 1% glutaraldehyde. The exosomes were contrasted and embedded with 4% uranyl-oxalate solution and methyl cellulose-UA. The grids were air-dried before they were placed under transmission electronic microscope at 80 kV to acquire images.

Study Approval—All of the protocols and experiments performed in mice were approved by the Yale University School of Medicine.

Statistical Analysis—Data are shown as means ± S.E. or S.D. as bars in the histograms. Differences were considered statistically significant if $p \leq 0.05$ by Student's *t* test.

RESULTS

Angiopoietin-2 Is Secreted via Exosomes—To determine whether Ang2 is secreted via exosomes, we followed a standard exosome isolation protocol (Fig. 1*A*) (26) to isolate exosomes from the media conditioned by wild type or adenoviral Ang2 transduced primary mouse lung endothelial cells. The total and free proteins were extracted by acetone precipitation from the supernatant after low speed (10,000 × *g*) centrifugation or after high speed (100,000 × *g*) centrifugation, respectively. The *top panel* of Fig. 1*B* shows Ang2 in the medium. Most of Ang2 was recovered in 100,000 × *g* pellet (Fig. 1*B*: compare *second* and *third panels*) suggesting its possible presence in exosomes. To confirm that the 100,000 × *g* pellet fraction contains exosomes, we looked for the presence of known exosomal proteins von Willebrand Factor, CD63, and syntenin (11). All of these were present in the 100,000 × *g* pellet, whereas the endoplasmic reticulum maker, calnexin, which is not present in exosomes, was absent in the pellet (Fig. 1*C*).

OptiPrep gradients have been utilized to purify and characterize exosomes based upon their unique density, which is different from that of other vesicles such as endoplasmic reticu-

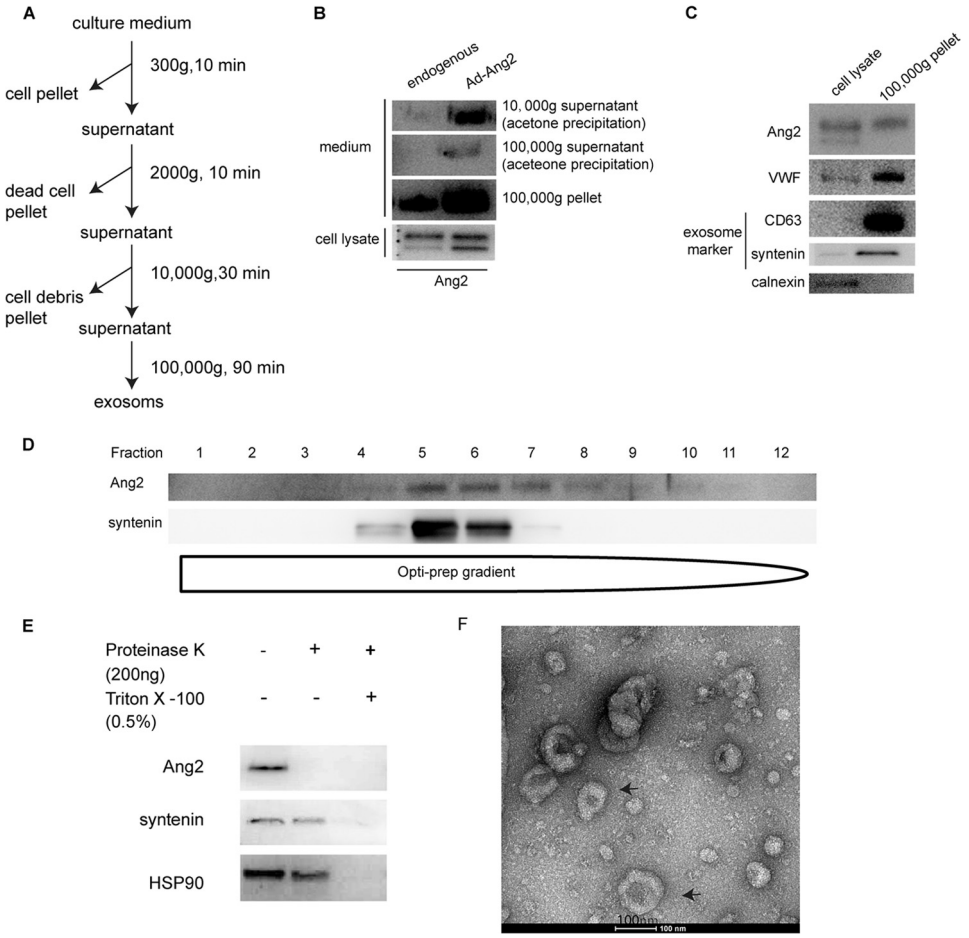

FIGURE 1. **Ang2 from endothelial cells is secreted on exosomes.** *A*, differential centrifugation protocol for the isolation of exosomes from culture media. *B*, Western blot analysis of Ang2 in cell lysates and media from HUVECs and HUVECs transduced with adenoviral Ang2 following differential centrifugation and precipitation. Note that the majority of Ang2 in the media is present in the 100,000 × *g* pellet fractions (P100) relative to the supernatant fraction (precipitated with acetone) following 100,000 × *g* ultracentrifugation. *C*, Western blot analysis of 100,000 × *g* pellet fractions with exosome markers. Note the enrichment of exosomal markers in the P100 fractions and absence of the endoplasmic reticulum marker calnexin. *D*, Western blot analysis of fractions from OptiPrep gradients (5–40%) of P100. Note that Ang2 co-sediments with the exosomal marker syntenin. *E*, Western blot analysis of P100 fractions treated with proteinase K in the presence or absence of Triton X-100. *F*, electron microscopy image of exosomes. A typical EM image of exosomes from mouse lung primary endothelial cells, note the "cup-shaped" morphology that is characteristic of exosomes. *Scale bar*, 100 nm.

lum and the Golgi (26). After exosomes were pelleted by ultracentrifugation at 100,000 × *g*, they were loaded onto an OptiPrep gradient for further separation. The fractions were analyzed by Western blotting. As shown in Fig. 1*D*, Ang2 from mouse primary lung endothelial cells co-sediments with syntenin, an exosome maker on Optiprep density gradients, demonstrating that Ang2 indeed is present in exosomes and ruling out the possibility that the Ang2 detected in the 100,000 × *g* fractions is contaminating free soluble protein.

To determine whether Ang2 exists on the surface or inside of exsomes, the exosome factions (100,000 × *g* pellet) were treated with proteinase K in the presence or absence of Triton X-100. Shown in Fig. 1*E*, Ang2 was digested both in the presence or absence of Triton X-100, whereas the other two exosome markers, which have previously been shown to be inside exosomes, were digested only in the presence of Triton X-100. This result suggests that Ang2 are on the surface of exosome.

Finally, we used electron microscopy to visualize exosomes isolated from the conditional medium of primary mouse lung endothelial cells. Structures with a characteristic cup-shaped morphology and size of 30–100 nm in diameter (26) were observed (Fig. 1*F*). Taken together, these results confirm that Ang2 is present in the exosomal fraction isolated from endothelial cell-conditioned medium.

The PI3K/Akt/eNOS Pathway Negatively Regulates the Secretion of Exosomal Ang2—Previous studies have reported that release of Ang2 is regulated by PTEN/PI3K/Akt pathway (7). Because Ang2 is known to exist in Weibel-Palade bodies (6), which also contain von Willebrand factor, and because the secretion of von Willebrand factor is regulated by NO (25), we hypothesized that the release of Ang2 might be also controlled by eNOS and its upstream regulators including Akt1 and PI3-kinase. To test this, we first investigated the release of exosomal Ang2 from lung endothelial cells isolated from *Akt1*$^{-/-}$ mice. The amount of Ang2 present in exosomes from the medium conditioned by *Akt1*$^{-/-}$ cells was significantly higher than in the supernatant conditioned by wild type (Akt1$^{+/+}$) endothelial cells (Fig. 2*A*), suggesting Akt1 negatively regulates Ang2 release. Syntenin levels were also increased in *Akt1*$^{-/-}$ cell-conditioned medium, indicating that deletion of Akt1 resulted in an increase in exosome biosynthesis rather than in specific elevation of Ang2 production (Fig. 2*A*). This was further con-

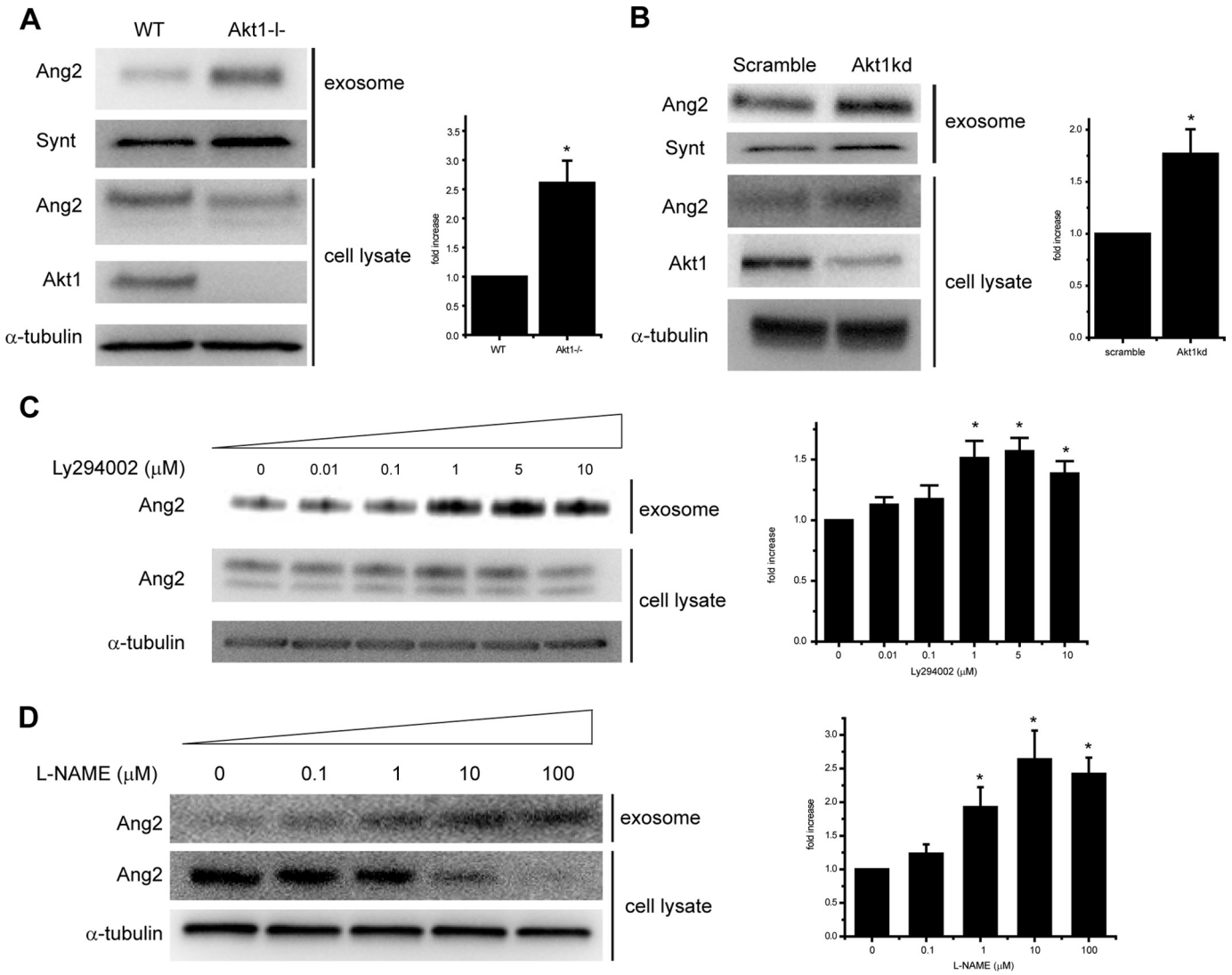

FIGURE 2. **Secretion of exosomal Ang2 is negatively regulated by the PI3K/AKT/eNOS pathway.** *A*, Western blot analysis of Ang2 in cell lysates and exosomes isolated from primary lung endothelial cells isolated from WT and Akt1$^{-/-}$ mice; quantification of Ang2 in exosomes (mean ± S.E.; *, $p < 0.05$). Note significant increase in Ang2 in exosomes isolated from Akt1$^{-/-}$ mice. *B*, Western blot analysis of Ang2 in cell lysates and exosomes isolated from HUVECs transfected with Akt1 siRNA; quantification of Ang2 in exosomes (mean ± S.E.; *, $p < 0.05$). Note significant increase in Ang2 in exosomes following Akt1 knockdown. *C*, Western blot analysis and quantification of exosomal Ang2 from WT ECs following treatment with various concentrations of the PI3K inhibitor LY294002 (mean ± S.E.; *, $p < 0.05$). Note significant increase in Ang2 in exosomes after PI3K inhibition. *D*, Western blot analysis and quantification of exosomal Ang2 from WT ECs following treatment with various concentrations of the eNOS inhibitor L-NAME (mean ± S.E.; *, $p < 0.05$). Note significant increase in Ang2 in exosomes after eNOS inhibition. *Synt*, syntenin.

firmed by siRNA knockdown of Akt1 in HUVECs that also led to an increase in exosomal Ang2 (Fig. 2*B*).

Next, we treated wild type lung endothelial cells with the PI3K inhibitor LY294002 and the Akt inhibitor L-NAME and examined their effect of on exosomal Ang2 release. Treatment with either inhibitor resulted in a dose-dependent increase in exosomal Ang2 levels in the conditioned media (Fig. 2, *C* and *D*). Taken together, these results point to PI3K/Akt/eNOS-dependent regulation of exosomal Ang2 release.

The Syndecan/syntenin Pathway Positively Regulates the Exosomal Ang2 Secretion—Syndecans and syntenin are essential for exosome biosynthesis (11). To evaluate the relative contribution of syndecan-4/syntenin to Ang2 secretion, we compared the secretion of Ang2 from the lung endothelial cells isolated from WT and syndecan-4$^{-/-}$ (*Sdc4*$^{-/-}$) mice. The Ang2 levels, both in total cell lysates and the exosome fraction, were significantly decreased in *Sdc4*$^{-/-}$ relative to wild type endothelial cells (Fig. 3*A*). Syntenin levels were reduced in syndecan-4$^{-/-}$ compared with WT endothelial cells (Fig. 3*A*), indicating that the decrease in Ang2 caused by deletion of syndecan-4 was due to a reduction in exosome biosynthesis. The decreased Ang2 levels in the cell lysates and exosome fraction of *Sdc4*$^{-/-}$ cells were significantly increased following transduction of these cells with an adenovirus containing full-length syndecan-4 (Fig. 3*B*), indicating that the presence of syndecan-4 is necessary for normal Ang2 production.

Syntenin binds to S4 via its phosphoinositol 4,5-bisphosphate and PDZ binding domains (14). Knockdown of syntenin by siRNA in HUVECs led to a significant decrease in Ang2 levels in both the exosomal fraction and in cell lysates (Fig. 3*C*). Because the PI3K/Akt1/eNOS and syndecan/syntenin pathways play opposing roles in the regulation of Ang2 levels, we next examined the effect of blocking both signaling systems on Ang2 release. We used siRNAs to knock down Akt1 and S4

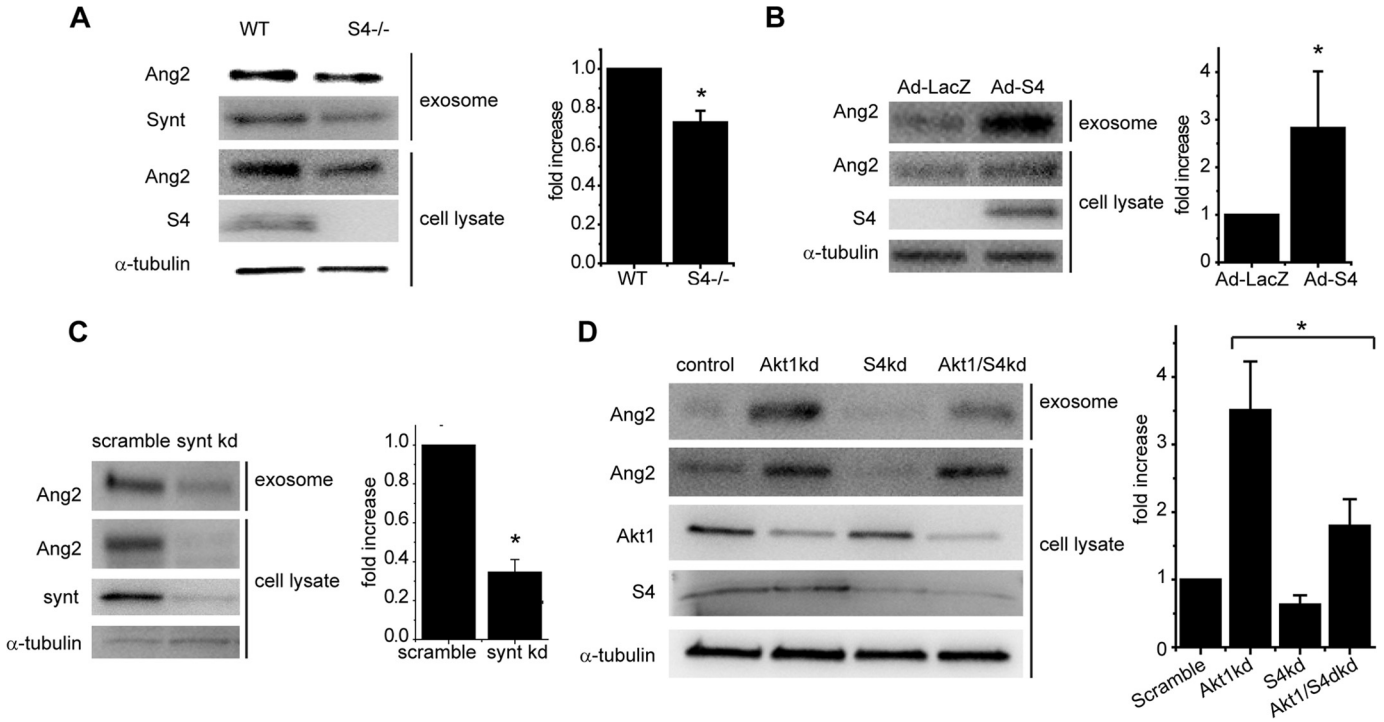

FIGURE 3. **Syndecan/syntenin controls secretion of exosomal Ang2.** *A*, Western blot analysis of Ang2 in cell lysates and exosomes isolated from primary lung endothelial cells isolated from WT and $S4^{-/-}$ mice; quantification of Ang2 in exosomes (mean ± S. E.; *, $p < 0.05$). Note the significant decrease in Ang2 in exosomes isolated from $Akt1^{-/-}$ mice. *B*, Western blot analysis of Ang2 in cell lysates and exosomes isolated from $S4^{-/-}$ ECs following transduction with control and adenoviral (*Ad*) S4 adenoviral constructs; quantification of Ang2 in exosomes (mean ± S.E.; *, $p < 0.05$). Note the significant increase in Ang2 in exosomes following restoration of S4 expression in $S4^{-/-}$ ECs. *C*, Western blot analysis of Ang2 in cell lysates and exosomes isolated from HUVECs treated with control or syntenin siRNA; quantification of Ang2 in exosomes (mean ± S.E.; *, $p < 0.05$). Note the significant decrease in Ang2 in lysates and exosomes in cells lacking syntenin. *D*, Western blot analysis of Ang2 in cell lysates and exosomes from HUVECs treated with control, Akt1, S4, or Akt1/S4 siRNAs and quantification of Ang2 in exosomes (mean ± S.E.; *, $p < 0.05$). Note that knockdown (*kd*) of Akt1 and syndecan-4 results in normal Ang2 levels in cell lysates and exosomes. *Synt*, syntenin.

separately or together in HUVECs. As shown in Fig. 3*D*, efficient siRNA knockdown was achieved in both cases. In agreement with previous results, knockdown of Akt1 increased exosomal Ang2 levels, whereas S4 knockdown had the opposite effect. At the same time, knockdown of S4 following Akt1 knockdown restored the exosomal Ang2 levels to almost control levels.

Decreased Density of Coronary Arterioles in the Postnatal Akt1 Knock-out Mice Can Be Rescued in the Akt1/S4 Double Knock-out Mice—Increased Ang2 levels would be expected to lead to disruption of vascular growth (3). To investigate a potential link between high release levels of Ang2 in $Akt1^{-/-}$ endothelial cells and low levels of its release in $S4^{-/-}$ endothelium, we evaluated vascular density in $Akt1^{-/-}$, $Sdc4^{-/-}$, and $Akt1^{-/-}/Sdc4^{-/-}$ mice. Micro-CT analysis of coronary vasculature at postnatal day 7 demonstrated significantly decreased arterial density in $Akt1^{-/-}$ compared with wild type mice (Fig. 4, *A* and *B*), whereas arteriolar density in $Sdc4^{-/-}$ mice was comparable with controls (Fig. 4, *A* and *C*). Remarkably, the $Akt1^{-/-}/S4^{-/-}$ DKO mice displayed a greater number of the smallest (<16 μm) coronary arterioles than the $Akt1^{-/-}$ mice, demonstrating a partial rescue of the decreased vessel density phenotype (Fig. 4, *A* and *D*).

Deletion of S4 Rescues Impaired Arteriogenesis in Akt1 Null Mice—Akt1 knock-out mice display defective blood flow recovery in the hind limb ischemia model (22). Because our *in vitro* data indicate that $Akt1^{-/-}$ endothelial cells secrete higher levels of exosomal Ang2, we reasoned that the blood flow recovery defect in Akt1 knock-out mice might, at least in part, be due to excessive Ang2 secretion and that decreasing secretion by deletion of S4 could rescue the phenotype. Consistent with the previous report (22), blood flow recovery was severely attenuated in $Akt1^{-/-}$ mice at all the time points compared with WT mice (Fig. 5, *A*–*C*), whereas no difference was seen between $S4^{-/-}$ and WT mice (Fig. 5, *A*–*C*). However, in the case of the $Akt1^{-/-}/Sdc4^{-/-}$ mice, despite an initial lag in the recovery of blood flow, by 28 days following surgery, the animals recovered to the same extent as $Sdc4^{-/-}$ mice.

S4/Akt1 Double Knock-out Rescues Delayed Retinal Vascular Development Caused by Akt1 Knock-out—We compared the vascular growth in retinas at neonatal day 5 in wild type, $Sdc4^{-/-}$, $Akt1^{-/-}$, and $Akt1^{-/-}/S4^{-/-}$ DKO mice. $Akt1^{-/-}$ mice retinas exhibited significantly delayed vascular growth, whereas $Sdc4^{-/-}$ mice retinas developed normally when compared with WT (Fig. 6, *A* and *B*). $Akt1^{-/-}/Sdc4^{-/-}$ DKO mice showed an insignificant decrease in retinal vascular development relative to controls but a significant increase above that seen in $Akt1^{-/-}$ mice (Fig. 6, *A* and *B*).

DISCUSSION

Angiopoietin-2 plays a multitude of roles in regulating blood and lymphatic vessel growth, maturation, remodeling and vascular permeability as well as inflammation. Despite numerous studies aimed at elucidating its function, mechanism of action,

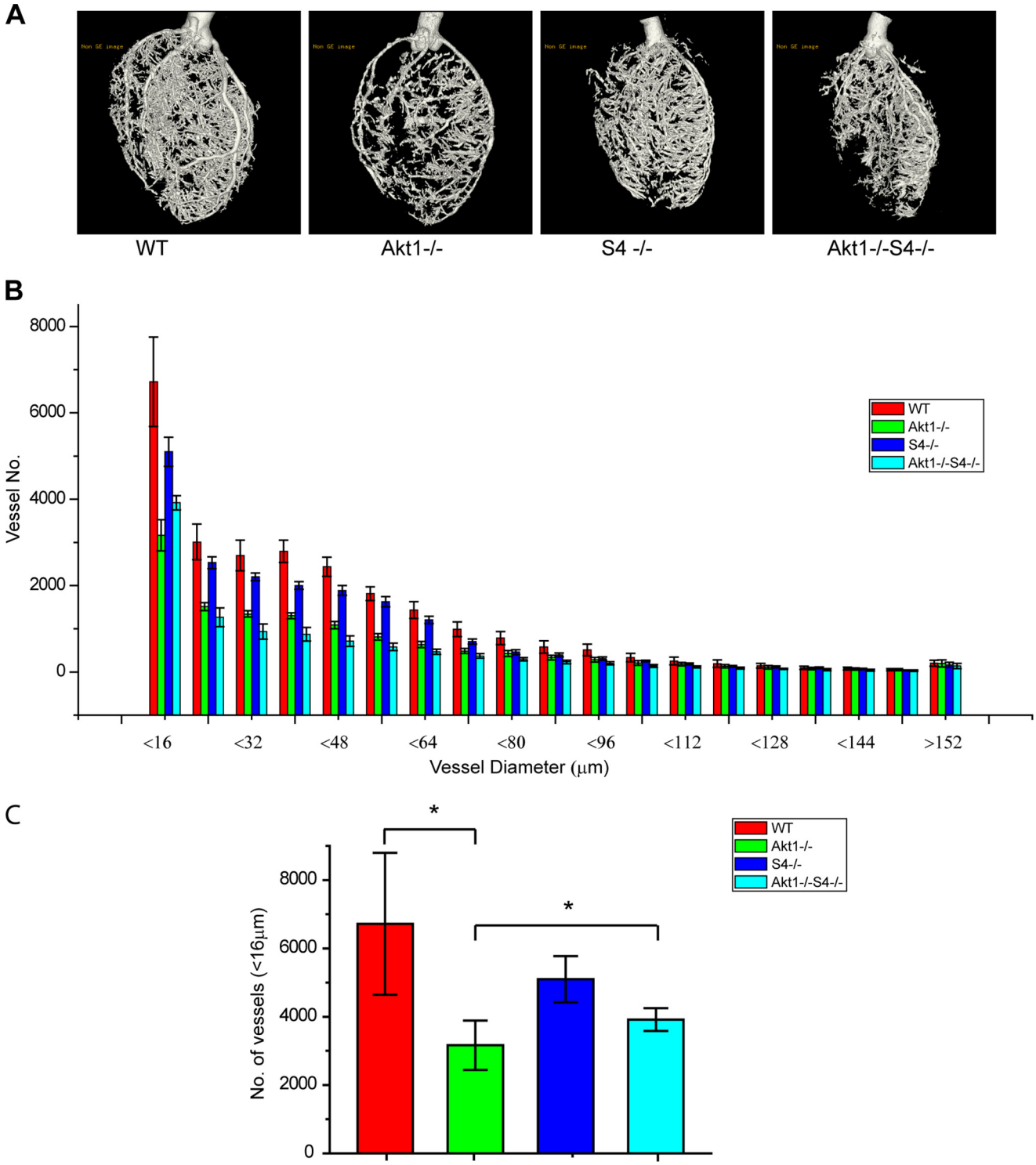

FIGURE 4. **Decreased blood vessel density in postnatal Akt1 KO mouse hearts and deletion of S4 partially rescues the Akt1 phenotype in postnatal hearts.** *A*, representative reconstructive micro-CT images of day 7 neonatal hearts from WT, Akt1$^{-/-}$, S4$^{-/-}$, and Akt1/S4 DKO mice at 16 μm resolution. *B*, quantitative analysis of micro-CT images from WT and Akt1 KO neonatal heart (mean ± S.E.; *, $p < 0.05$). *C*, quantitative analysis of micro-CT images from S4 KO and Akt1$^{-/-}$/S4$^{-/-}$ DKO neonatal heart (mean ± S.E.; *, $p < 0.05$). *D*, quantitative analysis of micro-CT images of vessels ≤ 16 μm in diameter from WT, Akt1$^{-/-}$, S4$^{-/-}$, and Akt1$^{-/-}$/S4$^{-/-}$ DKO neonatal heart (mean ± S.E.; *, $p < 0.05$). Note the significant decrease in the total number of ≤100-μm diameter vessels in Akt1$^{-/-}$ mice relative to WT and that S4$^{-/-}$ on the Akt1$^{-/-}$ background rescues the decrease in smaller vessels (≤16 μm) seen in Akt1$^{-/-}$ mice.

and regulation of expression, little is known regarding the factors regulating Ang2's release from endothelial cells. It seems unlikely that such a critically important secreted protein, such as Ang2, would be released in an unregulated manner. In this study, we provide evidence demonstrating that Ang2 is secreted from endothelial cells via exosomes and that this secretion is controlled by two pathways- PI3K/Akt/eNOS pathway negatively regulating the release and the syndecan/syntenin pathway providing positive regulation. In other words, inhibition of PI3K/AKT/eNOS signaling leads to an increase in exosomal

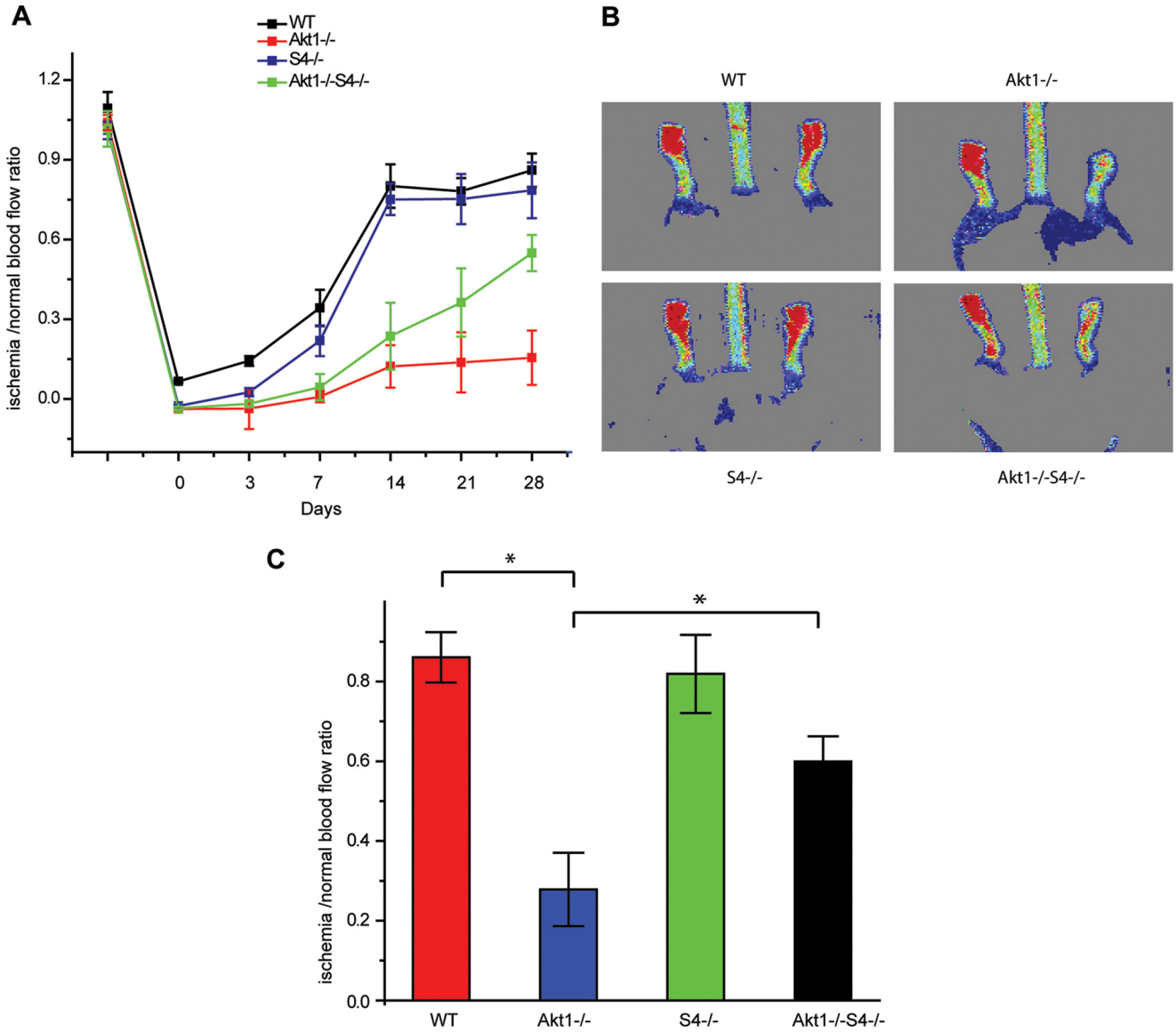

FIGURE 5. **Impaired blood flow recovery in Akt1$^{-/-}$ mice is rescued in Akt1$^{-/-}$/S4$^{-/-}$ DKO mice in the hind limb ischemia model.** *A*, quantitative analysis of laser Doppler after hind limb ischemia surgery of WT, Akt1$^{-/-}$, S4$^{-/-}$, and Akt1$^{-/-}$/S4$^{-/-}$ DKO mice, blood flow recovery was measured by mean perfusion expressed as a ratio of the surgically treated ischemic paw relative to the control paw (mean ± S.E.). *B*, representative laser Doppler images at day 28 from WT, Akt1$^{-/-}$, S4$^{-/-}$, and Akt1$^{-/-}$/S4$^{-/-}$ DKO mice. *C*, quantitative analysis of blood flow recovery 4 weeks after hind limb ischemia from WT, Akt1$^{-/-}$, S4$^{-/-}$, and Akt1$^{-/-}$/S4$^{-/-}$ DKO mice (mean ± S.E.; *, $p < 0.05$). Note that S4$^{-/-}$ on the Akt1$^{-/-}$ background restores hind limb perfusion following surgery.

Ang2 release, whereas reduction in S4 or syntenin expression results in reduced Ang2 release.

This conclusion is supported by several lines of evidence. In cell culture, Ang2 is clearly found on endosomes and not as a free protein, and its secretion is stimulated by any intervention that blocks PI3K/AKT/eNOS signaling. At the same time, a knock-out or knockdown of either syndecan-4 or syntenin blocks Ang2 release. *In vivo*, *Akt1*$^{-/-}$ mice display a number of vascular defects, including rarefication of the coronary arterial tree, impaired retinal vascular development, and impaired blood flow recovery in the hind limb model that are consistent with increased Ang2 secretion. Crossing *Akt1*$^{-/-}$ mice with *Sdc4*$^{-/-}$ mice partially restored these phenotypes. Thus, our data, both *in vitro* and *in vivo*, point to a crucial connection among three vital signaling pathways: PI3K/Akt/eNOS, Ang2, and syndecan/syntenin.

Our results extend previous studies that have pointed to the role of these molecules in Ang2 release. Tsigkos *et al.* (7) have shown that inhibition of PI3K and Akt increases Ang2 release, whereas Matsushita *et al.* (25) demonstrated that nitric oxide controls the exocytosis of Weiber-Palade bodies, and Fiedler *et al.* (6) showed that Ang2 is stored in Weiber-Palade bodies. All of these results are consistent with the data in the current study showing that Ang2 is released on endosomes in a PI3K/Akt/eNOS-dependent manner.

It was recently been shown that syndecans regulate biosynthesis of exosomes in epithelial cells via an interaction with syntenin (11). However, the biological significance of this regulation has not been fully explored. Here, we show that in endothelial cells Ang2 is one of the cargos in exosomes, located on their external surface, and that exosomal release of Ang2 is modulated by syndecan/syntenin. This finding expands the

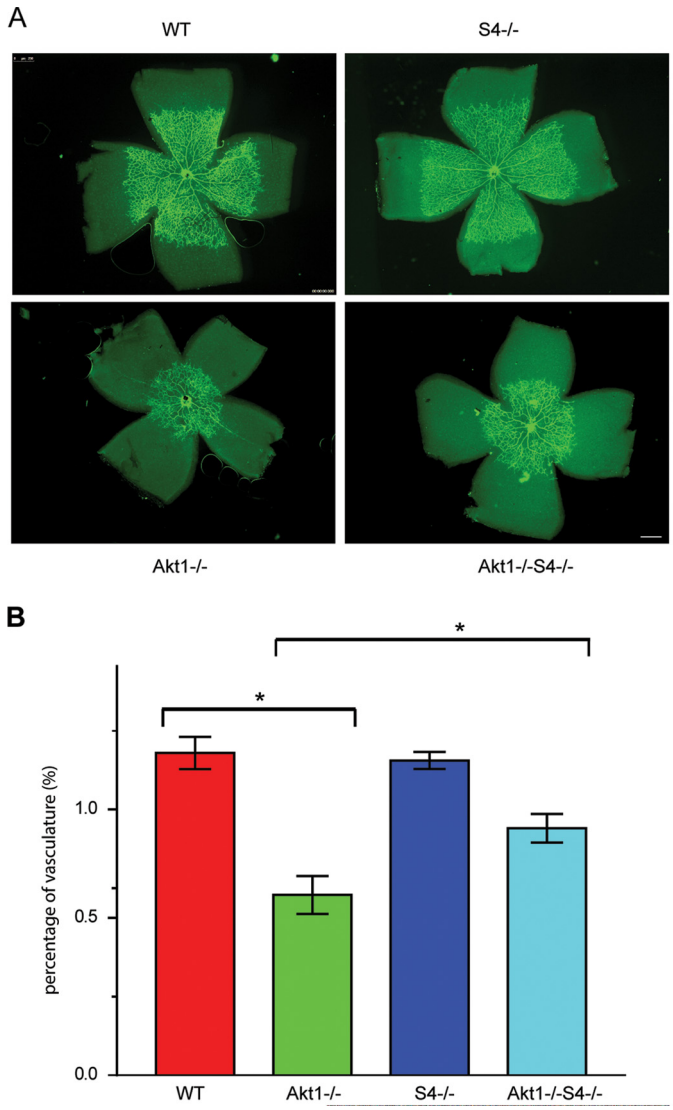

FIGURE 6. **Akt1$^{-/-}$/S4$^{-/-}$ DKO rescues delayed vascular development in Akt1$^{-/-}$ retina.** *A*, representative P5 retinas stained with isolectin B4 from WT, Akt1$^{-/-}$, S4$^{-/-}$, and Akt1$^{-/-}$/S4$^{-/-}$ DKO mice. *B*, quantitative analysis of vascular area *versus* avascular area of retinas from WT, Akt1$^{-/-}$, S4$^{-/-}$, and Akt1$^{-/-}$/S4$^{-/-}$ DKO mice (mean ± S.E.). *, $p < 0.05$. Note that the delayed retinal vascular development in Akt1$^{-/-}$ mice is rescued when S4$^{-/-}$ is crossed onto the Akt1$^{-/-}$ background.

functional role of syndecans and provides mechanistic insights into how syndecans might work with Ang2 to regulate vascular development and inflammation (31, 32).

It is worth noting that relative to the effect that blockade of the PI3K/Akt/eNOS pathway has on Ang2 release via exosomes, the effect of knock-out or knockdown of S4 on Ang2 release is rather modest. This is most likely due to the presence of multiple syndecan family members in endothelial cells. Baietti *et al.* (11) reported that double knockdown of syndecan-1 and syndecan-4 in epithelial cells (MCF-7) impaired the release of exosomes to a greater extent than knockdown of either alone. Consistent with this notion, we found that the knockdown of syntenin, which binds multiple syndecans, had a greater effect on Ang2 release than knock down of a single syndecan. It should be noted that S4 deletion has a larger impact when Ang2 levels are elevated, as is the case when the Akt1 levels are reduced.

In all three animal models we examined, deletion of *Sdc4* on the Akt1$^{-/-}$ background to generate the Akt1$^{-/-}$/Sdc4$^{-/-}$ DKO mouse resulted in partial but not complete rescue of the vascular defect. A likely explanation for the partial rescue is that there are multiple etiologies of vascular defects in Akt1$^{-/-}$ mice given the central role Akt1 signaling has in many cellular functions. Thus, reducing increased release of Ang2 corrects the phenotype only in part.

In summary, our study shows that the PI3K/Akt/eNOS and syndecan/syntenin pathways regulate exosomal Ang2 release in an opposing manner. Ang2 is thought to be an attractive therapeutic target for the treatment of cancer because combination of VEGF and Ang2-targeting therapies has shown improved efficacy against tumor growth compared with target either VEGF or Ang2 alone (33). The ability of syndecans to regulate the release of Ang2 may provide a novel target for compounds designed to regulate Ang2 levels. The observation that *Sdc4*$^{-/-}$ mice have minimal defects under normal physiological conditions suggests that a temporary blockade of syndecan activity may result in little or no side effects, thus increasing the appeal of syndecans as potential targets for regulating Ang2 levels in the treatment of cancer and other vascular pathologies.

Acknowledgment—We thank Filipa Moraes (Yale University) for help with retinal preparations.

REFERENCES

1. Augustin, H. G., Koh, G. Y., Thurston, G., and Alitalo, K. (2009) Control of vascular morphogenesis and homeostasis through the angiopoietin-Tie system. *Nat. Rev. Mol. Cell Biol.* **10,** 165–177
2. Suri, C., Jones, P. F., Patan, S., Bartunkova, S., Maisonpierre, P. C., Davis, S., Sato, T. N., and Yancopoulos, G. D. (1996) Requisite role of angiopoietin-1, a ligand for the TIE2 receptor, during embryonic angiogenesis. *Cell* **87,** 1171–1180
3. Maisonpierre, P. C., Suri, C., Jones, P. F., Bartunkova, S., Wiegand, S. J., Radziejewski, C., Compton, D., McClain, J., Aldrich, T. H., Papadopoulos, N., Daly, T. J., Davis, S., Sato, T. N., and Yancopoulos, G. D. (1997) Angiopoietin-2, a natural antagonist for Tie2 that disrupts in vivo angiogenesis. *Science* **277,** 55–60
4. Yuan, H. T., Khankin, E. V., Karumanchi, S. A., and Parikh, S. M. (2009) Angiopoietin 2 is a partial agonist/antagonist of Tie2 signaling in the endothelium. *Mol. Cell. Biol.* **29,** 2011–2022
5. Daly, C., Eichten, A., Castanaro, C., Pasnikowski, E., Adler, A., Lalani, A. S., Papadopoulos, N., Kyle, A. H., Minchinton, A. I., Yancopoulos, G. D., and Thurston, G. (2013) Angiopoietin-2 functions as a Tie2 agonist in tumor models, where it limits the effects of VEGF inhibition. *Cancer Res.* **73,** 108–118
6. Fiedler, U., Scharpfenecker, M., Koidl, S., Hegen, A., Grunow, V., Schmidt, J. M., Kriz, W., Thurston, G., and Augustin, H. G. (2004) The Tie-2 ligand angiopoietin-2 is stored in and rapidly released upon stimulation from endothelial cell Weibel-Palade bodies. *Blood* **103,** 4150–4156
7. Tsigkos, S., Zhou, Z., Kotanidou, A., Fulton, D., Zakynthinos, S., Roussos, C., and Papapetropoulos, A. (2006) Regulation of Ang2 release by PTEN/PI3-kinase/Akt in lung microvascular endothelial cells. *J. Cell. Physiol.* **207,** 506–511
8. Gross, J. C., Chaudhary, V., Bartscherer, K., and Boutros, M. (2012) Active Wnt proteins are secreted on exosomes. *Nat. Cell Biol.* **14,** 1036–1045
9. Théry, C. (2011) Exosomes: secreted vesicles and intercellular communications. *F1000 Biol. Rep.* **3,** 15
10. Hanson, P. I., and Cashikar, A. (2012) Multivesicular body morphogenesis.

Annu. Rev. Cell Dev. Biol. **28,** 337–362
11. Baietti, M. F., Zhang, Z., Mortier, E., Melchior, A., Degeest, G., Geeraerts, A., Ivarsson, Y., Depoortere, F., Coomans, C., Vermeiren, E., Zimmermann, P., and David, G. (2012) Syndecan-syntenin-ALIX regulates the biogenesis of exosomes. *Nat. Cell Biol.* **14,** 677–685
12. Choi, Y., Chung, H., Jung, H., Couchman, J. R., and Oh, E. S. (2011) Syndecans as cell surface receptors: Unique structure equates with functional diversity. *Matrix Biol.* **30,** 93–99
13. Gao, Y., Li, M., Chen, W., and Simons, M. (2000) Synectin, syndecan-4 cytoplasmic domain binding PDZ protein, inhibits cell migration. *J. Cell. Physiol.* **184,** 373–379
14. Grootjans, J. J., Zimmermann, P., Reekmans, G., Smets, A., Degeest, G., Dürr, J., and David, G. (1997) Syntenin, a PDZ protein that binds syndecan cytoplasmic domains. *Proc. Natl. Acad. Sci. U.S.A.* **94,** 13683–13688
15. Tkachenko, E., Elfenbein, A., Tirziu, D., and Simons, M. (2006) Syndecan-4 clustering induces cell migration in a PDZ-dependent manner. *Circ. Res.* **98,** 1398–1404
16. Elfenbein, A., Rhodes, J. M., Meller, J., Schwartz, M. A., Matsuda, M., and Simons, M. (2009) Suppression of RhoG activity is mediated by a syndecan 4-synectin-RhoGDI1 complex and is reversed by PKCα in a Rac1 activation pathway. *J. Cell Biol.* **186,** 75–83
17. Zimmermann, P., Zhang, Z., Degeest, G., Mortier, E., Leenaerts, I., Coomans, C., Schulz, J., N'Kuli, F., Courtoy, P. J., and David, G. (2005) Syndecan recycling [corrected] is controlled by syntenin-PIP2 interaction and Arf6. *Dev. Cell* **9,** 377–388
18. Morgan, M. R., Hamidi, H., Bass, M. D., Warwood, S., Ballestrem, C., and Humphries, M. J. (2013) Syndecan-4 phosphorylation is a control point for integrin recycling. *Dev. Cell* **24,** 472–485
19. Partovian, C., Ju, R., Zhuang, Z. W., Martin, K. A., and Simons, M. (2008) Syndecan-4 regulates subcellular localization of mTOR Complex2 and Akt activation in a PKCα-dependent manner in endothelial cells. *Mol. Cell* **32,** 140–149
20. Ju, R., and Simons, M. (2013) Syndecan 4 regulation of PDK1-dependent Akt activation. *Cell Signal* **25,** 101–105
21. Karar, J., and Maity, A. (2011) PI3K/AKT/mTOR Pathway in Angiogenesis. *Front Mol. Neurosci.* **4,** 51
22. Ackah, E., Yu, J., Zoellner, S., Iwakiri, Y., Skurk, C., Shibata, R., Ouchi, N., Easton, R. M., Galasso, G., Birnbaum, M. J., Walsh, K., and Sessa, W. C. (2005) Akt1/protein kinase Bα is critical for ischemic and VEGF-mediated angiogenesis. *J. Clin. Invest.* **115,** 2119–2127
23. Chen, J., Somanath, P. R., Razorenova, O., Chen, W. S., Hay, N., Bornstein, P., and Byzova, T. V. (2005) Akt1 regulates pathological angiogenesis, vascular maturation and permeability *in vivo*. *Nat. Med.* **11,** 1188–1196
24. Schleicher, M., Yu, J., Murata, T., Derakhshan, B., Atochin, D., Qian, L., Kashiwagi, S., Di Lorenzo, A., Harrison, K. D., Huang, P. L., and Sessa, W. C. (2009) The Akt1-eNOS axis illustrates the specificity of kinase-substrate relationships in vivo. *Sci. Signal.* **2,** ra41
25. Matsushita, K., Morrell, C. N., Cambien, B., Yang, S. X., Yamakuchi, M., Bao, C., Hara, M. R., Quick, R. A., Cao, W., O'Rourke, B., Lowenstein, J. M., Pevsner, J., Wagner, D. D., and Lowenstein, C. J. (2003) Nitric oxide regulates exocytosis by *S*-nitrosylation of *N*-ethylmaleimide-sensitive factor. *Cell* **115,** 139–150
26. Thery, C., Amigorena, S., Raposo, G., and Clayton, A. (2006) Isolation and characterization of exosomes from cell culture supernatants and biological fluids. *Current Protocols in Cell Biology*, pp. 30:3.22.1–3.22.29, Wiley and Sons, Hoboken, NJ
27. Ishiguro, K., Kadomatsu, K., Kojima, T., Muramatsu, H., Iwase, M., Yoshikai, Y., Yanada, M., Yamamoto, K., Matsushita, T., Nishimura, M., Kusugami, K., Saito, H., and Muramatsu, T. (2001) Syndecan-4 deficiency leads to high mortality of lipopolysaccharide-injected mice. *J. Biol. Chem.* **276,** 47483–47488
28. Cho, H., Thorvaldsen, J. L., Chu, Q., Feng, F., and Birnbaum, M. J. (2001) Akt1/PKBα is required for normal growth but dispensable for maintenance of glucose homeostasis in mice. *J. Biol. Chem.* **276,** 38349–38352
29. Tang, M., Li, J., Huang, W., Su, H., Liang, Q., Tian, Z., Horak, K. M., Molkentin, J. D., and Wang, X. (2010) Proteasome functional insufficiency activates the calcineurin-NFAT pathway in cardiomyocytes and promotes maladaptive remodelling of stressed mouse hearts. *Cardiovasc. Res.* **88,** 424–433
30. Zagorchev, L., Oses, P., Zhuang, Z. W., Moodie, K., Mulligan-Kehoe, M. J., Simons, M., and Couffinhal, T. (2010) Micro computed tomography for vascular exploration. *J Angiogenes. Res.* **2,** 7
31. Alexopoulou, A. N., Multhaupt, H. A., and Couchman, J. R. (2007) Syndecans in wound healing, inflammation and vascular biology. *Int. J. Biochem. Cell Biol.* **39,** 505–528
32. Fiedler, U., and Augustin, H. G. (2006) Angiopoietins: a link between angiogenesis and inflammation. *Trends Immunol.* **27,** 552–558
33. Gerald, D., Chintharlapalli, S., Augustin, H. G., and Benjamin, L. E. (2013) Angiopoietin-2: an attractive target for improved antiangiogenic tumor therapy. *Cancer Res.* **73,** 1649–1657